

# Universality of Jamming Criticality in Overdamped Shear-Driven Frictionless Disks Supplemental Material

Daniel Vågberg,<sup>1</sup> Peter Olsson,<sup>1</sup> and S. Teitel<sup>2</sup>

<sup>1</sup>*Department of Physics, Umeå University, 901 87 Umeå, Sweden*

<sup>2</sup>*Department of Physics and Astronomy, University of Rochester, Rochester, NY 14627*

(Dated: June 30, 2014)

## TRANSVERSE VELOCITY CORRELATION FUNCTION

The one quantity for which models RD<sub>0</sub> and CD<sub>0</sub> are clearly different is the transverse velocity correlation function,  $g_y(x) \equiv \langle v_y(0)v_y(x) \rangle$ . Defining the normalized correlation,  $G_y(x) \equiv g_y(x)/g_y(0)$ , we plot in Fig. 1(a)  $G_y(x)$  vs  $x$ , for several different values of strain rate  $\dot{\gamma}$ , for model RD<sub>0</sub> at  $\phi = 0.8433 \approx \phi_J$  in a system of  $N = 4096$  particles. We see that  $G_y(x)$  has a clear minimum at a distance  $x = \ell$ , and that  $\ell$  increases as  $\dot{\gamma} \rightarrow 0$  and one approaches the critical point. In Ref. [1]  $\ell$  was interpreted as the diverging correlation length  $\xi$ . In CD<sub>0</sub> however, it was found [2] that  $G_y(x)$  decreases monotonically without any obvious strong dependence on either  $\phi$  or  $\dot{\gamma}$ . In Fig. 1(b) we plot  $G_y(x)$  vs  $x$ , for several different  $\dot{\gamma}$ , at  $\phi = 0.8433 \approx \phi_J$  in a system of  $N = 4096$  particles, confirming this result.

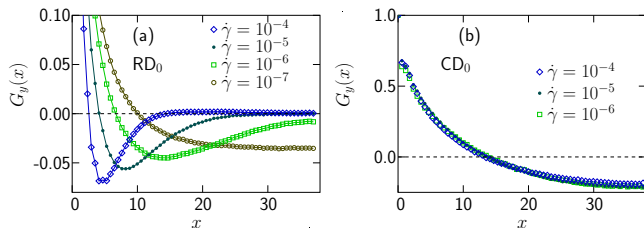


FIG. 1. Normalized transverse velocity correlation function  $G_y(x) = g_y(x)/g_y(0)$  at  $\phi = 0.8433 \approx \phi_J$  for a system of  $N = 4096$  particles. Panel (a) is for model RD<sub>0</sub> with shear rates  $\dot{\gamma} = 10^{-7}$  through  $10^{-4}$ . Panel (b) for model CD<sub>0</sub> at shear rates  $\dot{\gamma} = 10^{-6}$ , through  $10^{-4}$ .

As an alternative way to consider the difference in this correlation between the two models, we now consider the Fourier transformed correlation  $g_y(k_x) = \int dx g_y(x)e^{ik_x x}$ , which we show in Figs. 2(a) and 2(b) for RD<sub>0</sub> and CD<sub>0</sub> respectively at packing fraction  $\phi = 0.8433 \approx \phi_J$ . For RD<sub>0</sub> we see a maximum in  $g_y(k_x)$  at a  $k_x^*$  that decreases for decreasing  $\dot{\gamma}$ ;  $\ell \sim 1/k_x^*$  gives the corresponding minimum of the real-space correlation. For CD<sub>0</sub> we show results only for the single strain rate  $\dot{\gamma} = 10^{-6}$  since from Fig. 1(a) we expect no observable difference as  $\dot{\gamma}$  varies. We see an algebraic divergence  $g_y(k_x) \sim k_x^{-1.3}$  as  $k_x \rightarrow 0$ . It is this algebraic divergence that causes the real space  $G_y(x)$  in CD<sub>0</sub> to become solely a function of  $x/L$  as the system length  $L$  increases, as was

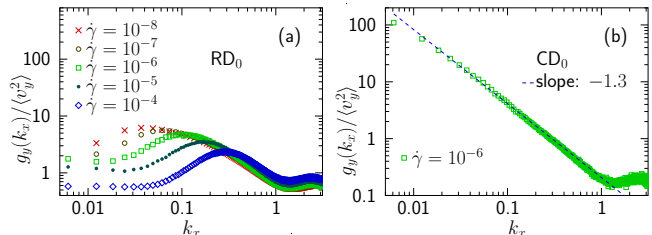


FIG. 2. Fourier transform of the transverse velocity correlation function  $g_y(k_x)$  at  $\phi = 0.8433 \approx \phi_J$ . Panel (a) is for model RD<sub>0</sub> with shear rates  $\dot{\gamma} = 10^{-8}$  through  $10^{-5}$ . The peak in  $g_y(k_x)$ , moving to smaller  $k_x$  as  $\dot{\gamma}$  decreases, is related to the minimum in the real space  $g_y(x)$  moving to larger  $x$ . The algebraic behavior in panel (b) for model CD<sub>0</sub> at  $\dot{\gamma} = 10^{-6}$ , is consistent with the absence of any apparent length scale, as reported in Ref. [2]. The number of particles in these figures are  $N = 262144$  except for the two smallest shear rates for RD<sub>0</sub> for which  $N = 65536$ .

reported in Ref. [2].

To try and give a qualitative understanding of this differing behavior of  $g_y(k_x)$ , we can consider how energy is dissipated in each model. In RD<sub>0</sub> the dissipation is  $(1/N) \sum_i \langle |\delta \mathbf{v}_i|^2 \rangle \approx \int d\mathbf{k} \langle \delta \mathbf{v}(\mathbf{k}) \cdot \delta \mathbf{v}(-\mathbf{k}) \rangle$ . For CD<sub>0</sub>, however, the dissipation is  $(1/N) \sum_{i,j} \langle |\mathbf{v}_i - \mathbf{v}_j|^2 \rangle \approx \int d\mathbf{k} \langle \delta \mathbf{v}(\mathbf{k}) \cdot \delta \mathbf{v}(-\mathbf{k}) \rangle |\mathbf{k}|^2$ , where the sum is over only neighboring particles  $i, j$  in contact. Here  $\delta \mathbf{v}$  is the non-affine part of the particle velocity. If we make an equipartition-like ansatz, and assume that as  $k \rightarrow 0$  all modes  $\mathbf{k}$ , and both spatial directions  $x, y$ , contribute equally to the dissipation, we would then conclude that for RD<sub>0</sub>  $\langle v_y(\mathbf{k})v_y(-\mathbf{k}) \rangle \propto \text{constant}$ , while for CD<sub>0</sub>  $\langle v_y(\mathbf{k})v_y(-\mathbf{k}) \rangle \propto 1/k^2$ . Noting that  $g_y(k_x) = \int dk_y \langle v_y(\mathbf{k})v_y(-\mathbf{k}) \rangle$ , we then conclude that for RD<sub>0</sub> we have  $g(k_x) \propto \text{constant}$  as  $k_x \rightarrow 0$ , while for CD<sub>0</sub> we have the divergence  $g(k_x) \propto 1/k_x$ . This saturation of  $g_y(k_x)$  for RD<sub>0</sub>, as compared to the algebraic divergence of  $g_y(k_x)$  for CD<sub>0</sub>, is what is qualitatively seen in Fig. 2.

The physical reason for this dramatic difference can be viewed as follows. For CD<sub>0</sub>, since the dissipation depends only on velocity differences, uniform translation of a large cluster of particles with respect to the ensemble average flow has little cost, thus enabling long wavelength fluctuations. For RD<sub>0</sub> the dissipation is with respect to a fixed background, so uniform translation of a large cluster causes dissipation that scales with the cluster size; long wavelength fluctuations are suppressed.

That the observed divergence in  $CD_0$  is  $\sim k_x^{-1.3}$  rather than the simple  $k_x^{-1}$  predicted above, suggests that our equipartition ansatz is not quite correct, and that the different modes interact in a non-trivial way. That the exponent of this divergence is not an integer or simple rational fraction suggests the signature of underlying critical fluctuations, even though the correlation  $g_y(x)$  itself does not yield any obvious diverging length scale.

### FINITE-SIZE-SCALING OF PRESSURE

In Fig. 1 of the main article we showed data for the dependence of pressure  $p$  on system size  $L$  at different strain rates  $\dot{\gamma}$ , at the jamming fraction  $\phi_J \approx 0.8433$ . We argued that these results provided evidence for a similar growing, macroscopically large, correlation length  $\xi$  in both models  $RD_0$  and  $CD_0$ . Here we attempt a finite-size-scaling analysis of this data. We must note at the outset, however, that our earlier work [3] demonstrated that it is important to consider corrections-to-scaling to get accurate values for the exponents at criticality, and that corrections-to-scaling are in fact large at the smaller sizes  $L$  considered in Fig. 1 of the main article [4]. Since our data for  $p(L)$  is not extensive enough to try a scaling analysis including corrections-to-scaling, our results based on a fit to Eq. (5) must be viewed as providing only *effective* exponents describing the data over the range of parameters considered, rather than the true exponents asymptotically close to criticality. We restate Eq. (5),

$$p(\phi_J, \dot{\gamma}, L) = L^{-y/\nu} \mathcal{P}(0, \dot{\gamma}L^z). \quad (1)$$

We can equivalently write the above in the form

$$p(\phi_J, \dot{\gamma}, L) = \dot{\gamma}^{y/z\nu} f(L\dot{\gamma}^{1/z}), \quad (2)$$

using  $f(x) \equiv x^{-y/\nu} \mathcal{P}(0, x^z)$ . We can now adjust the parameters  $q \equiv y/z\nu$  and  $z$  to try and collapse the data to a single common scaling curve. Plotting  $p/\dot{\gamma}^q$  vs  $L\dot{\gamma}^{1/z}$  we show the results for  $RD_0$  and  $CD_0$  in Figs. 3(a) and (b). For  $RD_0$  we find the effective exponents  $z = 6.5$  and  $q = 0.290$ , while for  $CD_0$  we find  $z = 6.0$  and  $q = 0.317$ . The values of  $z$  found in the present analysis are comparable to the value  $z = 5.6$  found in the cruder analysis in Fig. 1(b) of the main article. Note that for both models the scaling function  $f(x) \rightarrow \text{constant}$  as  $x \rightarrow \infty$ , which gives  $p \sim \dot{\gamma}^q$ ,  $q \equiv y/z\nu$ , in the limit of an infinite sized system.

The closeness of these fitted *effective* exponents for the two models is one more piece of evidence that  $RD_0$  and  $CD_0$  behave qualitatively the same, and do not have dramatically different rheology as was claimed by Tighe et al. in Ref. [2].

Finally we consider how the effective exponents found here compare to the true exponents asymptotically close to criticality. From our most accurate analysis [3] of

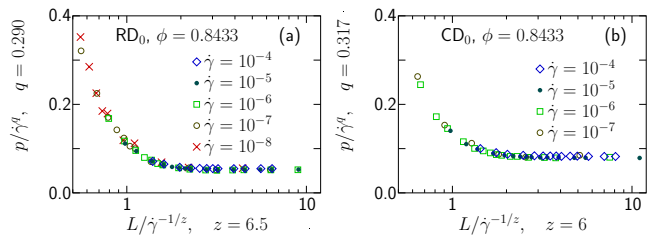


FIG. 3. Scaling collapse of pressure according to Eq. (2) for models  $RD_0$  and  $CD_0$ .

the critical behavior in  $RD_0$ , using a large system size  $N = 65536$  and including the leading corrections-to-scaling, we have found the critical exponents  $q = y/z\nu = 0.28 \pm 0.02$  and  $y = 1.08 \pm 0.03$ , yielding  $z\nu = 3.9 \pm 0.4$ . This value of  $q$  is in reasonable agreement with that found above from the finite-size-scaling analysis of  $p(\phi_J, \dot{\gamma}, L)$ . If we take the value of  $z \approx 6$  found in the finite-size-scaling analysis, we would then conclude  $\nu \approx 0.65$ . We note that earlier scaling analyses [1, 5] that similarly ignored corrections-to-scaling found similar values for  $\nu$ . However our recent [4] more detailed finite-size-scaling analysis of the correlation length exponent, which included corrections-to-scaling, found that  $\nu \approx 1$ , therefore implying  $z \approx 3.9$  as the true critical value. We thus conclude that the larger than expected value of  $z$  found here from the finite-size-scaling of  $p$  is due to the strong corrections-to-scaling that effect the correlation length at small  $L$ .

As another way to see the effect of corrections-to-scaling on the correlation length, in Fig. 4 we plot our results for  $p$  vs  $L$  at  $\phi = 0.8433 \approx \phi_J$ , as obtained from quasistatic simulations [4, 6] representing the  $\dot{\gamma} \rightarrow 0$  limit. From Eq. (1) we expect as  $\dot{\gamma} \rightarrow 0$  the behavior,  $p \sim L^{-y/\nu}$ . If we fit the data at small  $L$  in Fig. 4 to a power law, we then find the exponent,  $y/\nu \approx 1.79$ . Using  $y = 1.08$  this then gives  $\nu \approx 0.60$ , in rough agreement with the value of  $\nu$  obtained from the measured  $z$  of our finite-size-scaling of  $p$  with  $\dot{\gamma}$ . If, however, we fit the data at only the largest  $L$  to a power law, we then find the exponent  $y/\nu \approx 1.11$ . Again using  $y = 1.08$ , we then get  $\nu \approx 0.97$ , in better agreement with the expected  $\nu \approx 1$ . Fig. 4 thus shows in a very direct way that corrections-to-scaling are significant for small system lengths  $L$ .

To conclude this section, although our finite-size-scaling of the pressure data in Fig. 1(a) of the main article is effected by corrections-to-scaling, and so gives a larger value for the dynamic exponent  $z$  than we believe is actually the case at criticality, nevertheless the correlation length  $\xi$  extracted from this data and shown in Fig. 1(b) demonstrates that  $RD_0$  and  $CD_0$  are behaving qualitatively the same, and that both have a macroscopic length scale  $\xi$  that is growing (and we would argue diverging) as the jamming transition is approached.

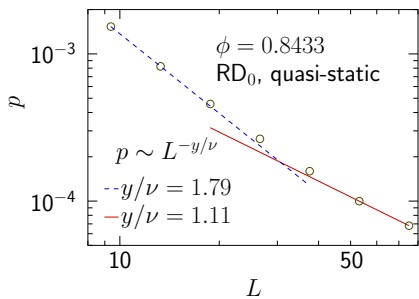


FIG. 4. Pressure  $p$  vs system length  $L$  at  $\phi_J \approx 0.8433$  for quasistatic shearing. Dashed line is a power law fit to the data at the smallest  $L$ , giving an exponent  $y/\nu \approx 1.79$ ; solid line is a power law fit to the data at the largest  $L$ , giving an exponent  $y/\nu \approx 1.11$ .

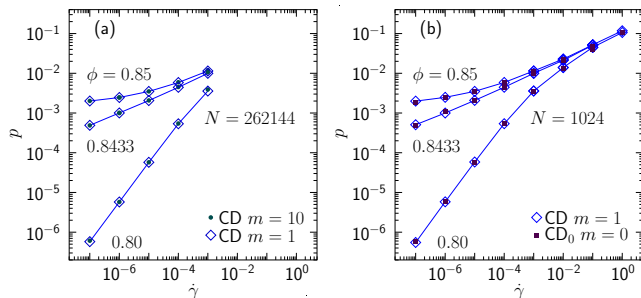


FIG. 5. Pressure  $p$  vs. shear strain rate  $\dot{\gamma}$  at packing fractions  $\phi = 0.80, 0.8433, 0.85$  for: (a) model CD with  $m = 1$  and  $m = 10$  for  $N = 262144$  particles, and (b) model CD with  $m = 1$  and model  $CD_0$  with  $m = 0$  for  $N = 1024$  particles.

## EFFECT OF FINITE MASS ON MODEL CD

We wish to verify that the mass parameter  $m = 1$ , which we use in model CD, is indeed sufficiently small so as to put our results in the overdamped  $m \rightarrow 0$  limit corresponding to model  $CD_0$ , for the range of parameters studied here. In Fig. 5(a) we show results for the elastic part of the pressure  $p$  vs  $\dot{\gamma}$  for model CD, with  $N = 262144$  particles, at three different packing fractions:  $\phi = 0.80$ ,  $\phi = 0.8433 \approx \phi_J$ , and  $\phi = 0.85$ . We compare results for two different mass parameters,  $m = 1$  and  $m = 10$ . We see that the results agree perfectly for small  $\dot{\gamma}$ ; significant differences are only found for  $\dot{\gamma} \geq 10^{-3}$  which is higher than the largest shear rate used in our scaling analysis. In Fig. 5(b) we similarly compare results for model CD with  $m = 1$  with explicit results for model  $CD_0$ , as obtained from simulations using the more costly matrix inversion dynamics for  $m = 0$ . In this case we are restricted to  $N = 1024$  particles because our algorithm for  $CD_0$  scales as  $N^2$ . We see that in all cases there is no observed difference between the two models. Thus we conclude that our results from CD with  $m = 1$  are indeed in the overdamped  $m \rightarrow 0$  limit.

- 
- [1] P. Olsson and S. Teitel, Phys. Rev. Lett. **99**, 178001 (2007).
  - [2] B. P. Tighe, E. Woldhuis, J. J. C. Remmers, W. van Saarloos, and M. van Hecke, Phys. Rev. Lett. **105**, 088303 (2010).
  - [3] P. Olsson and S. Teitel, Phys. Rev. E **83**, 030302(R) (2011).
  - [4] D. Vågberg, D. Valdez-Balderas, M. A. Moore, P. Olsson, and S. Teitel, Phys. Rev. E **83**, 030303(R) (2011).
  - [5] C. S. O'Hern, L. E. Silbert, A. J. Liu, and S. R. Nagel, Phys. Rev. E **68**, 011306 (2003).
  - [6] D. Vågberg, P. Olsson, and S. Teitel, Phys. Rev. E **83**, 031307 (2011).